Residual stress and pinch contributions to momentum transport in JET neutral beam heated H-modes

H. Weisen[1], Y. Camenen[2], A. Salmi[3], M. Gelfusa[4] and JET-EFDA contributors*

JET-EFDA, Culham Science Centre, Abingdon, OX14 3DB, UK
[1]Centre de Recherches en Physique des Plasmas, EPFL, 1015 Lausanne, Switzerland
[2] PIIM UMR 7345, Aix-Marseille Université / CNRS, Marseille, France
[3]Association EURATOM-Tekes, VTT, Finland
[4]Associazione EURATOM-ENEA-University of Rome "Tor Vergata", Roma, Italy

**see the Appendix of F. Romanelli et al, Proc 24th IAEA Fusion Energy Conference 2012, San Diego, USA*

1. INTRODUCTION.

The existence of non-diffusive momentum transport can be considered as firmly established from transient transport analysis in several devices [1-4]. In NBI driven JET H-modes, the existence of a pinch has been established both using NBI modulation techniques [2] and using database analysis [3,4], with consistent results. Comparisons of the observations with linear gyrokinetic calculations using the GKW code [5,6] have shown similar parameter scalings with R/L_n, q and $\varepsilon=r/R$, allowing the pinch to be identified as the theoretically predicted Coriolis pinch [6], but predicted pinch magnitudes are on the whole lower than observed. Several effects may be responsible for this difference: 1) systematic errors on the current profile reconstruction introducing a bias in the gyrokinetic modeling, 2) a difference between Carbon rotation (measured) and bulk ion rotation (predicted), 3) the presence of residual stresses (RS), 4) simplifying assumptions used in the gyrokinetic modeling in [3,4], namely the assumption of electrostatic fluctuations, a circular geometry and the simple quasi-linear estimate for the ratio of heat and momentum fluxes. In order to address these points, the present work introduces several refinements into a subset of the data presented in [3,4], which are all from the JET Carbon wall phase (before 2010). It uses EFIT equilibria constrained by polarimetry and allowing for finite edge pressure and current. Torque and heat deposition profiles are calculated using the ion orbit code ASCOT [7] for all samples in the subset, thereby taking into account any classical fast ion transport. All gyrokinetic simulations are repeated with the improved magnetic equilibrium and electromagnetic perturbations. Last, but not least, the difference in neoclassical rotation velocity between the measured impurity (C^{6+}) velocity and that of the main ion species (D^+) is calculated using the NEOART code [8].

2. JETPEAK DATABASE

The database approach relies on deriving scaling coefficients for the normalised angular frequency gradient $R/L_{\omega D}$, based on the time-independent dimensionless momentum balance equation [3,4].

$$R/L_{\omega D} = -\frac{\chi_i}{\chi_\phi}\left\{\frac{Rt}{\chi_i l} - \frac{R\Gamma_N}{\chi_i n_i}\right\} + \frac{RV}{\chi_\phi} + \frac{R\tau_{rs}}{\chi_\phi l} \qquad (1)$$

Here t is the local torque surface density (N/m) from NBI, $l=m_i n_i R^2 \omega_D$ is the angular momentum density, m_i the average ion mass, n_i the ion density, R the average major radius of the flux surface under consideration, ω_D the toroidal angular velocity of the main ions (Deuterium), Γ_N is the particle flux associated with the NBI particle source, χ_ϕ is the radial momentum diffusivity, V is the momentum pinch velocity, and τ_{rs} refers to RS contributions (N/m). The relevant plasma parameters, of which the main ones are shown in the table below, were sampled for 7 values of $\varepsilon=r/R$ in stationary conditions, corresponding to $0.25 \le r/a \le 0.85$.

	$\lvert t_i^*-\Gamma_N^*\rvert$	u	$R/L_{\omega D}$	R/L_n	R/L_{Ti}	R/L_{Te}	T_i/T_e	ε	ν_{eff}	β	ρ_i^*	q	s
min	0.03	0.15	0	0	3	3	0.6	0.075	0.06	0.001	7×10^{-4}	0.6	0
max	9	0.5	13	10	13	15	2.1	0.255	3	0.05	4×10^{-3}	5	5

Table: Dimensionless parameter ranges in JETPEAK H-mode database subset presented here and across the minor radius for $0.25 \le \rho \le 0.85$. Here $u=R\omega_D/v_i=R\omega_D/(2T_i/m_i)^{1/2}$ is the main ion Mach number, $L_{\omega D}=\omega_D/\nabla\omega_D$ etc, $\nu_{eff}=10^{-14}RZ_{eff}n_eT_e^{-2}$ is the collisionality, β is the local normalised thermal plasma pressure, $\rho_i^* = (2T_i/m_i)^{1/2}/(\omega_{ci}R)$ is the ion Larmor radius normalised to R, q is the local safety factor and $s=\varepsilon R/L_q$.

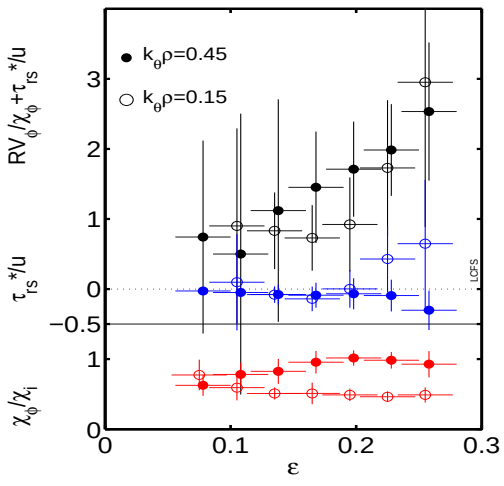

Fig.1 Profiles of transport parameters from linear, electromagnetic, collisional GKW simulations in realistic geometry. The residual stress contribution to $R/L_{\omega D}$ shown here (blue symbols) only includes the up-down asymmetry stress.

Three linear electromagnetic GKW calculations per sample and per radial position were performed in order to determine the Prandtl number χ_ϕ/χ_i, the pinch number RV/χ_ϕ and the up/down asymmetry RS [9] with input parameters from the experimental database. The dominant instability is found to be an ITG mode, although microtearing modes appear in 20% of the cases. Fig.1 shows, for two characteristic wavenumbers, the profiles of the ranges of χ_ϕ/χ_i (bottom, red) and of the total non-diffusive contribution to R/L_ω (top, black). The dots represent averages over the dataset and the bars span a standard deviation. The

contribution of the up-down asymmetry RS, $\tau_{rs}*/u=R\tau_{rs}/(\chi_\phi l)$, shown in blue, is very small. Evaluation of the more important contributions of RS resulting from $E\times B$ shearing from non-linear codes is planned, but beyond the scope of this paper.

3. CALCULATION OF DEUTERIUM ROTATION PROFILES

For comparison with the experiment, the D^+ rotation profiles must be obtained, based on the measured C^{6+} profiles. In [3,4], $\omega_D=\omega_C$ was assumed, whereas in this work the difference between D^+ and C^{6+} rotation is taken to be neoclassical. i.e. of the order of the diamagnetic velocity, with the D^+ ion rotation velocity more in the co-current direction than the C^{6+} rotation. We note that recent experimental results may challenge the assumption that the differential rotation between D^+ and C^{6+} is of purely neoclassical origin [10]. The neoclassical rotation difference is evaluated with the NEOART code [8] based on the experimental kinetic profiles for e^-, D^+ and C^{6+}, the magnetic equilibrium and the loop voltage as inputs.

Carbon, the dominant light impurity species in this dataset, contributes $\Delta Z_{eff}\sim 0.5$, as measured by CXRS. Visible Bremsstrahlung measurements however provide $Z_{eff}\sim 2.2$ on average. In order to deal with this discrepancy and test the sensitivity to the carbon density profile measurements, we calculate the NC correction with the following four assumptions:

1) CXRS carbon density profile at face value, carbon is sole contributor to Z_{eff}
2) Carbon assumed to contribute 70% of $<Z_{eff}>$ from vis. Brems., R/L_{nC} from CXRS
3) as 2), but $R/L_{nC} = R/L_{nD} = R/L_{ne}$ obtained from Thomson Scattering
4) Carbon assumed to contribute 70% of $<Z_{eff}>$ from vis. Brems, $R/L_{nC} = 0$

Fig.2 shows a typical example of an angular frequency profile for C^{6+}, together with the inferred D^+ rotation profiles, in the above cases. The rotation velocity of D^+ is significantly larger than for C^{6+}, especially near the edge, leading to smaller normalised angular frequency gradients (fig.3). The smallest changes from the C^{6+} rotation profiles are obtained in cases 1 and 2, which we believe to be the most realistic.

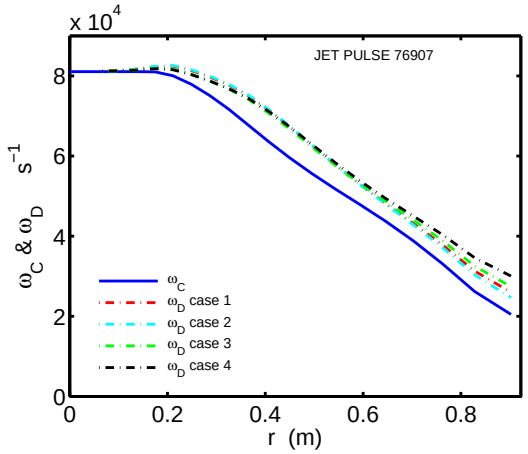

Fig.2 Angular frequency profiles for C^{6+} and D^+

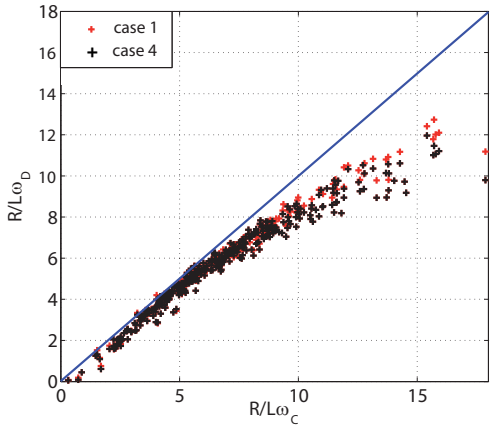

Fig.3 $R/L_{\omega D}$ versus $R/L_{\omega C}$ for cases 1 and 4

4. DISCUSSION

From theory [6], we expect the pinch to dominate over RS when $O_{rs}=\rho_i^*(R/L_{Ti})^2/u<<1$. O_{rs} spans a range between ~0.01 and 0.6, the highest values being obtained near the edge. Fig.4 shows, for case 1) at r/a=0.85, the scaling of $R/L_{\omega D}$ with torque term in eq.(1), compactly written as t_i^*-Γ_N^*. A regression of the form $R/L_{\omega D}=\chi_i/\chi_\phi\,(t_i^*-\Gamma^*)+VR/\chi_\phi+c_{rs}O_{rs}$ is performed in order to determine any scaling with O_{rs}, which may indicate the presence of RS, and a pinch number unaffected by RS. The symbols represent classes of O_{rs}, the lines showing the regressed scaling of $R/L_{\omega D}$ with t_i^*-Γ_N^* for $O_{rs}=0$ (red —) and $O_{rs}=0.6$ (blue·-), the latter representing the largest value of O_{rs}. Fig.5 shows typical profiles of transport coefficients, with $c_{rs}\langle O_{rs}\rangle=\tau_{rs}^*/u$, the inferred average contribution of RS to $R/L_{\omega D}$ in blue. No significant scaling with O_{rs} is found throughout the minor radius in all four cases, leading us to conclude that there is no significant RS contribution for r/a≤0.85. Note that, as a result of correlations between O_{rs} and ω_D-ω_C, omitting the correction for differential rotation leads to the incorrect conclusion that significant RS is present for the highest values of O_{rs}. Fig.5 shows a similar increase of RV/χ_ϕ with minor radius as seen fig.1 for GKW predictions, but with a larger magnitude. Future comparisons with non-linear GKW calculations and with a recent version of TGLF [11], may help resolving this discrepancy.

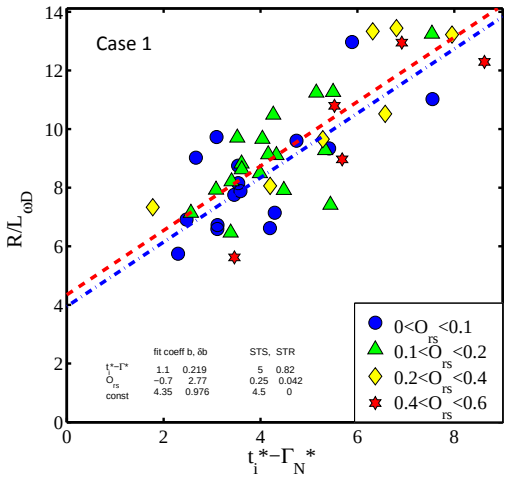

Fig.4 Scaling of $R/L_{\omega D}$ with net dimensionless torque at r/a=0.85 and regression coefficients.

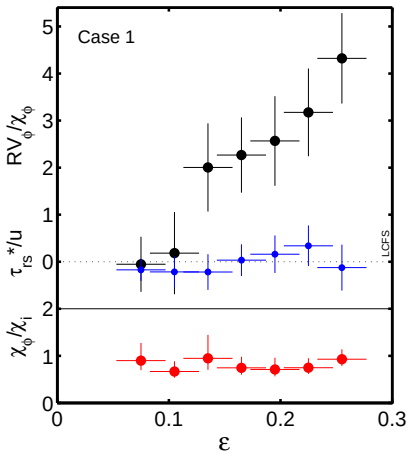

Fig.5 From top to bottom: Profiles of average pinch number, average residual stress contribution and Prandtl number.

References

[1] M. Yoshida et al, 2012, NF **52** 123005

[2] T. Tala et al, 2011, NF **51** 123002,

[3] H. Weisen et al, 2012, NF **52** 042001

[4] H. Weisen et al, 2012, NF **52** 114024

[5] A.G. Peeters, 2009,CPC **180**, 2650

[6] A. Peeters et al, 2011, NF **51**, 094027

[7] J.A. Heikkinen et al, 2001, J. Comp. Phys. **173** 527

[8] A.G. Peeters, 2000 Phys. Plasmas 7 268

[9] Y. Camenen et al, 2009, Phys. Rev. Lett. **102** 125001

[10] B. Grierson et al, 2012, Phys. Plasmas **19** 056107

[11] G. M. Staebler et al, 2013, PRL **110** 055003